# The MYST Family Histone Acetyltransferase Sas3 Governs Diverse Biological Processes in *Aspergillus fumigatus*

Jae Yoon Kwon , Young-Ho Choi , Min-Woo Lee , Jae-Hyuk Yu * , Kwang-Soo Shin *

Posted Date: 8 November 2023

doi: 10.20944/preprints202311.0353.v1

Keywords: Aspergillus fumigatus; histone acetyltransferase; MYST family; Sas3; asexual development; stress responses; virulence; transcriptomics

*Article*

# The MYST Family Histone Acetyltransferase Sas3 Governs Diverse Biological Processes in *Aspergillus fumigatus*

**Jae Yoon Kwon [1], Young-Ho Choi [1], Min-Woo Lee [2], Jae-Hyuk Yu [3,*] and Kwang-Soo Shin [1,*]**

[1] Department of Microbiology, Graduate School, Daejeon University, Daejeon 34520, Korea; kjywodbs98@edu.dju.ac.kr (J.Y.K); youngho1107@gmail.com (Y.-H.C.); shinks@dju.kr (K.-S.S.)
[2] Soonchunhyang Institute of Medi-bio Science, Soonchunhyang University, Chungcheongnam-do 31151, Korea; mwlee12@sch.ac.kr (M.-W.L.)
[3] Department of Bacteriology, University of Wisconsin-Madison, Madison, WI 53706, USA; jyu1@wisc.edu (J.-H.Y.)
* Correspondence: shinks@dju.kr (K.-S.S.); jyu1@wisc.edu (J.-H.Y.); Tel.: +82-42-280-2439 (K.-S.S.); +1-608-262-4696 (J.-H.Y.); Fax: +82-42-280-2608 (K.-S.S.); +1-608-262-2976 (J.-H.Y.)

**Abstract:** The conserved MYST proteins form the largest family of histone acetyltransferases (HATs) that acetylate lysines within the N-terminal tails of histone, enabling active gene transcription. Here, we have investigated the biological and regulatory functions of the MYST family HAT Sas3 in the opportunistic human pathogenic fungus *Aspergillus fumigatus* using a series of genetic, biochemical, pathogenic, and transcriptomic analyses. The deletion (Δ) of *sas3* results in drastically reduced colony growth, asexual development, spore germination, response to stresses, and the fungal virulence. Genome-wide expression analyses have revealed that the Δ*sas3* mutant showed 2,402 significant differentially expressed genes; 1,147 up-regulated and 1,255 down-regulated. The representative up-regulated gene resulting from Δ*sas3* is hacA predicted to encode a bZIP transcription factor, whereas the UV-endonuclease UVE-1 was significantly down-regulated by Δ*sas3*. Furthermore, our Western blot analyses suggest that Sas3 likely catalyzes acetylation of H3K9, K3K14, and H3K29 in *A. fumigatus*. In conclusion, Sas3 is associated with diverse biological processes and can be a potential target for controlling pathogenic fungi.

**Keywords:** *Aspergillus fumigatus*; histone acetyltransferase; MYST family; Sas3; asexual development; stress responses; virulence; transcriptomics

## 1. Introduction

Protein acetylation is a conserved evolutionary modification that occurs in eukaryotes and prokaryotes and was first discovered in histones [1,2]. Histone acetyltransferases (HATs) catalyze acetylation of lysine residues within the N-terminal tails of histone proteins. This modification neutralizes the positive charge of lysines and results in transcriptionally active chromatin structure, enabling active gene transcription [3].

Based on locations and functions, HATs are classified into two categories. Type A HATs are located in the nucleus, and they acetylate nucleosomal histones, while type B HATs are cytoplasmic enzymes that acetylate newly synthesized histones leading to their transport from the cytoplasm to the nucleus. Type A HATs can be further divided into five families on the basis of the homology of conserved motifs; GNAT (Gcn5-related N-acetyltransferases), MYST (MOZ, YBF2/Sas3, Sas2, and TIP60), p300/CBP (CREB-binding protein), basal transcription factors, and nuclear receptor coactivators [4]. Among them, GNAT, MYST, and the p300/CBP family, have been well-studied in filamentous fungi.

MYST is one of the largest HAT family, mediate a diverse variety of biological functions, and preferentially acetylate histones H2A, H3, and H4 [5]. The MYST family include MOZ (monocytic leukemia zinc-finger protein), YBF2 (yeast binding factor 2), Sas2 (something about silencing 2), Sas3 (something about silencing 3), and TIP60 (Tat interactive protein-60) proteins and have high

 doi:10.20944/preprints202311.0353.v1



conserved sequence in the acetyl-CoA binding and zinc finger regions [6]. The most studied MYST histone acetyltransferases in fungi are Esa1 (essential Sas2-related acetyltransferase 1), Sas2, and Sas3. Sas3 is a catalytic subunit of the NuA3 (nucleosomal acetyltransferase of histone H3) complex and responsible for H3 acetylation [7].

In the plant pathogenic and aflatoxigenic fungus *Aspergillus flavus*, MystA (the Sas2 orthologue) and MystB (the Sas3 orthologue) have opposite functions in sclerotia formation and aflatoxin B1 (AFB1) production, where MystA plays a negative role and MystB plays a positive role [8]. In *Fusarium graminearum*, Sas3 is indispensable for the acetylation of H3K4, while Gcn5 is essential for the acetylation of H3K9, H3K18, and H3K27. Both are required for DON biosynthesis and pathogenicity [9]. The deletion of *sas3* in *Magnaporthe oryzae* has a significant effect on asexual differentiation, spore germination, and appressorium formation [10]. Deletion of *hat1* (*sas3* homolog) in the insect pathogen *Metarhizium robertsii*, results in a decrease in global H3 acetylation and activation of orphan secondary metabolite genes [11]. Mst2 (Sas3 orthologue) of another insect pathogen, *Beauveria bassiana* has shown to regulate global gene transcription through H3K14 acetylation, which enables regulating multiple stress responses and plays an essential role in sustaining the biological control potential against pests [12].

Further evidence of histone acetylation in human fungal pathogens was observed in *Histoplasma capsulatum*, *Cryptococcus neoformans*, and *A. fumigatus* [13–15]. However, in *A. fumigatus*, it have been reported only the function of GNAT family HATs [15,16]. So, we examined the functions of MYST family HAT, Sas3 and its influence on development, response to stresses, and pathogenesis. Furthermore, we analysed the transcriptome of the wild type (WT) and the deletion mutant to gain insight into the possible roles of Sas3.

## 2. Materials and Methods

### *2.1. Strains and Media*

All *A. fumigatus* strains used in this study were derivatives of the WT Af293 strain [17]. Fungal strains were grown on yeast extract-glucose medium (YG), glucose minimal medium (MMG) or MMG with 0.1% yeast extract (MMY) and appropriate supplements, as described previously [18].

### *2.2. Construction of Mutant Strains*

The deletion construct generated by double-joint PCR [19] containing the *A. nidulans* selective marker *AnipyrG* with the 5′ and 3′ flanking regions of the *A. fumigatus sas3* gene (AFUA_4g10910) was introduced into the recipient strains [20]. The selective marker was amplified from *A. nidulans* FGSC A4 genomic DNA. The complemented strain was also generated by double-joint PCR method [19] with *hygB* as a selective marker. The null mutants and complemented strains were confirmed by diagnostic PCR (using primer pair oligo1497/1498) followed by restriction enzyme digestion (Figure S1). The oligonucleotides used in this study are listed in Table S1.

### *2.3. Nucleic Acid Manipulation andAnalyses*

Total RNA was isolated as previously described [21]. RT-qPCR was performed using One-Step RT-PCR SYBR Mix (Doctor Protein, Seoul, Korea) and a Rotor-Gene Q real-time PCR system (Qiagen, Hilden, Germany). The amplification of a specific target DNA was verified by melting curve analysis. The expression ratios were normalized to the expression level of the endogenous reference gene *ef1α* [22,23] and calculated by the $2^{-\Delta\Delta Cq}$ method [24]. The expression stability of *ef1α* and efficiencies of PCRs of the target genes were determined, as previously described [25]. Expression levels of target gene mRNAs were analyzed using appropriate oligonucleotide pairs (Table S1). For RNA-seq analyses, total RNA was extracted and submitted to eBiogen, Inc. (Seoul, Korea) for library preparation and sequencing.

### *2.4. PhenotypeAnalyses*

 doi:10.20944/preprints202311.0353.v1



Radial growth was assayed by inoculation of spores in the center of appropriate media and measurement of colony diameters. Conidial production was quantified from two inoculation methods. Point-inoculated cultures were used as per the growth area and overlay-inoculated cultures were used on each plate. Conidia were collected using 0.5% Tween 80 solution, filtered through Miracloth (Calbiochem, San Diego, CA, USA), and counted using a hemocytometer. To test for cell wall and oxidative stress, calcofluor white (CFW), Congo red, SDS (0.02%), menadione (MD), and $H_2O_2$ were added to the YG media after autoclaving. Then conidia ($1 \times 10^5$) of relevant strains were inoculated into stressors treated media and incubated at 37 °C, and measured colony diameters. UV light tolerance test was carried out as described previously [26]. Briefly, fresh conidia were plated out on YG plates (100 conidia per plate). The plates were then irradiated immediately with UV using a UV cross-linker and incubated at 37°C for 48 h. The colony numbers were counted and calculated as a ratio of the untreated control.

*2.5. Enzyme Assay and Western Blot Analysis*

PKA activity was detected with previous method using PepTag® Non-Radioactive cAMP-Dependent Protein Kinase Assay kit (Promega, Madison, WI, USA) [27]. Catalase activity was visualized by negative staining with ferricyanide [28,29]. SOD activity was determined as the inhibition of nitroblue tetrazolium reduction [30]. For Western blotting, histone was extracted with Histone Extraction Kit (Abcam, ab113476, Cambridge, UK), according to manufacturer's manual. Approximately 50 μg of nuclear protein extract was electrophoresed on a 10% SDS-PAGE gel and subsequently electroblotted to nitrocellulose membranes. Relevant histone modifications were detected with primary antibodies specific to histone H3 (ab1791), H3acK4 (ab176799), H3acK9 (ab177177), H3acK14 (ab203952), H3acK18 (ab40888) and H3acK27 (ab4729) antibodies. Relative intensities of the enzyme activities and Western blot were quantified using the Image J 1.52k software (NIH, Bethesda, MD, USA).

*2.6. Virulence and Phagocytosis Assay*

The virulence assay was conducted, as previously described [25]. Briefly, the CrlOri: CD1 (ICR) (Orient Bio Inc., Seongnam, Korea) female mice (6–8 weeks old, weighing 30 g) were immunosuppressed by the treatment with cyclophosphamide and cortisone. Mice were intranasally infected with $1 \times 10^7$ conidia (10 mice per each fungal strain) suspended in 30 μL of 0.01% Tween 80 in PBS. Then mice were monitored every 12 h for 8 days after the challenge. Control mice were inoculated with sterile 0.01% Tween 80 in PBS. For histology experiments, the mice were sacrificed at 3 day after conidia infection. Kaplan–Meier survival curves were analyzed using the log-rank (Mantel–Cox) test for significance. A phagocytic assay was performed according to a modified method [31,32]. The MH-S cell lines were maintained in RPMI 1640 containing 10% fetal bovine serum (Invitrogen, Carlsbad, CA) and 50 μM of 2-mercaptoethanol (Sigma, St. Louis, MO, USA). The MH-S cells were adhered to coverslips in 6-well plates at a concentration of $5 \times 10^5$ cells/mL for 2 h and subsequently challenged with $1.5 \times 10^6$ conidia for 1 h. Unbound conidia were removed by washing with PBS and then incubated for 2 h at 37 °C in an atmosphere of 5% $CO_2$. Wells were then washed with PBS and observed with microscopy. The percentage of phagocytosis was assessed.

*2.7. Bioinformatic Analyses*

The amino acid sequences of *A. fumigatus* Sas3 was retrieved from the *A. fumigatus* Af293 genomic database (http://www.aspergillusgenome.org/) and dbHimo (hme.riceblast.snu.ac.kr/). Amino acid sequences of full length of Sas3 was subject to the SMART program (http://smart.embl-heidelberg.de) for structural comparison. The possible 3D structure was estimated using AlphaFold Protein Structure Database (http://alphafold. ebi.ac.uk/) based on the amino acid sequences.

*2.8. Statistics*

Preprints (www.preprints.org) | NOT PEER-REVIEWED | Posted: 8 November 2023 doi:10.20944/preprints202311.0353.v1



All experiments performed in triplicate and $p < 0.05$ was considered a significant difference. Data were expressed as mean ± standard error. GraphPad Prism 4 (GraphPad Software, Inc., San Diego, CA, USA) was used for the statistical analyses and graphical presentation of survival curve.

## 3. Results

### *3.1. Summary of A. fumigatus Sas3*

The estimated 3D structure (Figure 1A) and domain architectures (Figure 1B) of the Sas3 protein are shown in Figure 1. As shown, the MOZ_SAS domain is located in the central region and the N- and C- terminal segments flank the catalytic core. The predicted *A. fumigatus* Sas3 consists of 1,058 amino acids (aa) and has a MOZ_SAS domain (549 ~ 724 aa) and the two plant homeodomains (PHD) (203 ~ 229 aa, 452 ~ 528 aa). The amino acid sequence of the MOZ_SAS domain in *A. fumigatus* shows 96.0~100% identity with those of other *Aspergillus* species. On the other hand, the MOZ-SAS domain of *Saccharomyces cerevisiae* and *Candida albicans* show low similarity, 63.4% and 72.4 %, respectively, to that of *A. fumigatus*. Possible active site is glutamate (red in Figure 1C).

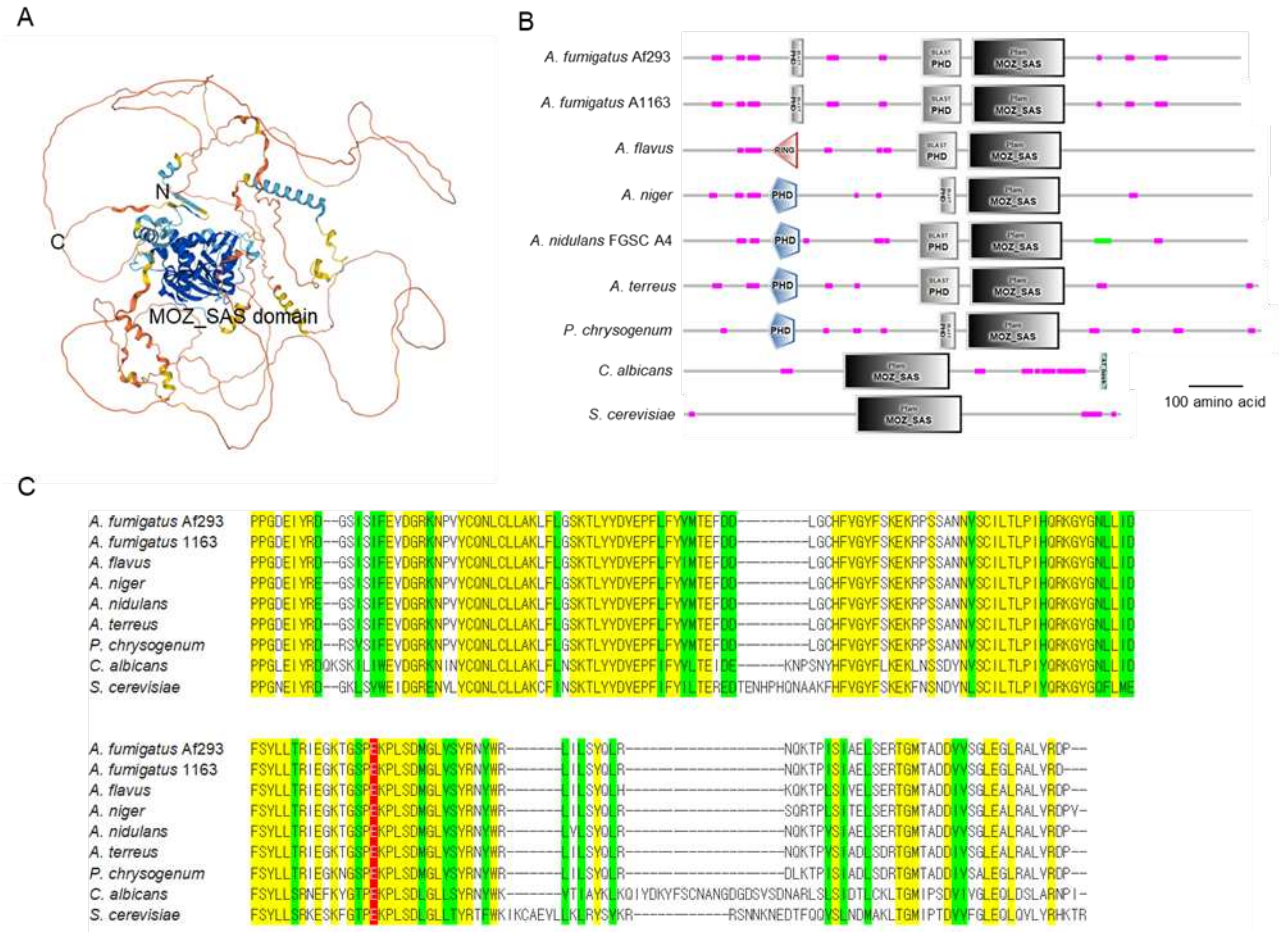


**Figure 1.** Domain architecture of the Sas3 protein. (A) A possible 3D structure of Sas3 protein estimated by AlphaFold Protein Structure Database (http://alphafold. ebi.ac.uk/) based on the amino acid sequences. (B) A domain structure of the Sas3 and Sas3 orthologs in various fungal species. Domain structures are presented using SMART (http://smart.embl-heidelberg.de). (C) Multiple sequence alignment of the MOZ_SAS domains of Sas3 and Sas3 orthologs. Yellow represents conserved residues, while green represents chemically similar residues. Red represents possible active site, respectively.

### *3.2. Sas3 is Required for Proper Growth and Development*

Preprints (www.preprints.org) | NOT PEER-REVIEWED | Posted: 8 November 2023 doi:10.20944/preprints202311.0353.v1



To investigate biological functions of Sas3, we generated the *sas3* null (Δ) mutant by employing DJ-PCR. As shown in Figure 2A, when grown on MMY and YG medium, the Δ*sas3* mutant colony displayed significantly reduced colony diameter (65%) compared to those of WT and complemented strain (*sas3* C) colonies). Moreover, our quantitative analyses of the number of asexual spores (conidia) per growth area and per plate have revealed that the number of conidia of the Δ*sas3* mutant was significantly decreased to about 23% (per growth area) and 77% (per plate) compared to those of WT and complemented strains (Figure 2B). Based on these results, we examined mRNA levels of the central asexual development regulators *abaA*, *brlA*, and *wetA* from the fungal cultures grown in MMY for 3 days. We found that the Δ*sas3* mutant showed highly reduced mRNA levels of all three activators of conidiation (Figure 2C). These results indicate that Sas3 plays a pivotal role in governing growth and asexual development in *A. fumigatus*.

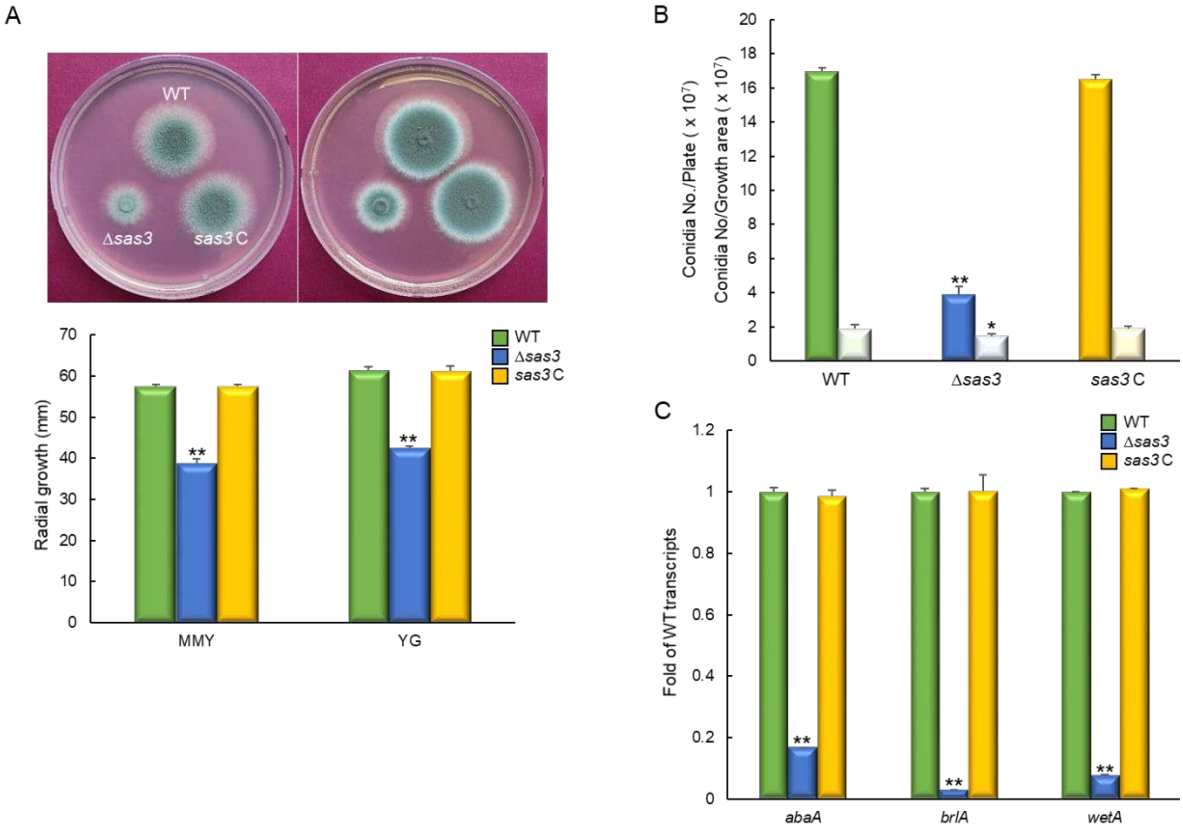


**Figure 2.** Roles of Sas3 in vegetative growth and asexual development. (A) Colony photographs of WT, Δ*sas3*, and *sas3* C strains point-inoculated and grown in solid MMY and YG medium. Radial growth of three strains grown on solid media for 3 days determined by colony diameter. (B) Conidia numbers produced by each strain per plate (dark color) and per growth area (light color). (C) Transcript levels of the key asexual developmental regulators in the mutants and complemented strains relative to those in WT at 3 days determined by quantitative RT-PCR (RT-qPCR). Fungal cultures were grown in MMY, and mRNA levels were normalized to the expression level of the *ef1α* gene. Statistical significance of differences was assessed by Student's *t*-test: * $p < 0.05$, ** $p < 0.01$.

### *3.3. Sas3 Positively Affects PKA Signaling Pathway and Spore Germination*

As the cAMP-dependent protein kinase A (PKA) singling pathway affects fungal spore germination, growth and development, we investigate the relationship between Sas3 and PKA by examining phosphorylation levels of the peptide substrate kemptide, which is specifically recognized and phosphorylated by PKA. The phosphorylated negatively charged kemptide migrates to the anode and the signal is proportional to higher PKA activity. The Δ*sas3* mutant showed lower PKA activity compare WT and *sas3* C strains (Figure 3A). To investigate the role of Sas3 in governing spore germination, we analyzed the kinetics of germ tube emergence in three strains. The germination rate

Preprints (www.preprints.org) | NOT PEER-REVIEWED | Posted: 8 November 2023 doi:10.20944/preprints202311.0353.v1



of the Δ*sas3* mutant was greatly decreased (Figure 3B). We also analyzed mRNA levels of PKA signaling components, *acyA* and *pkaC1*. As shown in Figure 3C, *acyA* and *pkaC1* mRNA levels were significantly lower in the Δ*sas3* mutant than in WT and *sas3* C strains. These results indicate that Sas3 is necessary for proper PKS signaling, which is associated spore germination, proliferation, and development of the fungus.

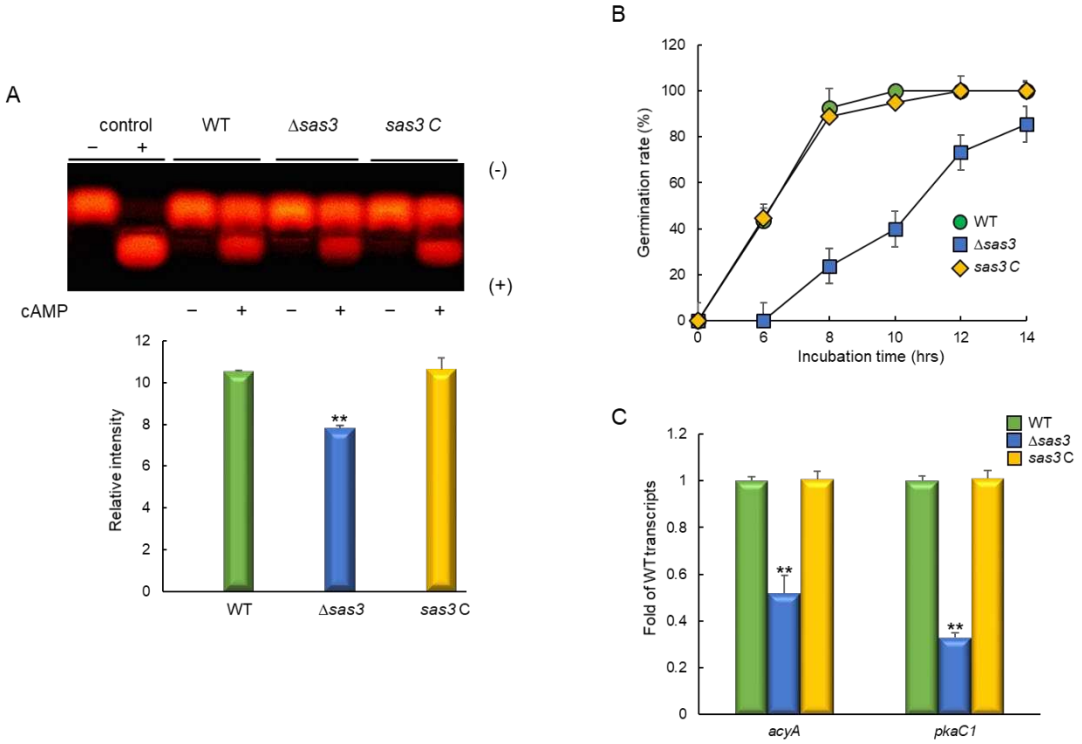


**Figure 3.** Sas3 affects the cAMP-PKA signaling pathway and spore germination. Sas3 affect sensitivity to cell wall perturbing agents. (A) PKA activity levels of three strains as monitored by gel electrophoresis. (B) Germination rate of spores. Conidia were inoculated in MMY and incubated at 37°C for 14 h. (C) Expression levels of *acyA* and *pkaC1* mRNA in WT, Δ*sas3*, and complemented (*sas3* C) strains analyzed by RT-qPCR. Statistical differences between strains were evaluated by Student's *t*-test: ** $p < 0.01$.

### *3.4. Sas3 is Involved in Cell Wall Stress Response*

We examined the effects of cell wall stressors on the growth of these strains by exposing them to cell wall stress compounds, calcofluor white (CFW), Congo red (CR), and SDS. The Δ*sas3* mutant exhibited significantly increased resistance to Congo red and SDS than WT and *sas3* C strain (Figure 4A). These findings suggest that cell wall composition and/or integrity may be affected by the loss of *sas3*. We further analyzed mRNA levels of the key chitin biosynthetic genes, *chsB*, *chsE*, and *gfaA*. When induced with Congo red (50 μg/mL, for 6 h), the mRNA levels of *chsB* and *chsE* were significantly decreased in mutant strain compared with WT and *sas3* C strain. In contrast, the mRNA expression level of *gfaA* was markedly increased by the loss of *sas3* (Figure 4B). Previously it had been demonstrated that the mRNA level of *gfaA* was increased by the treatment of cell wall stressors [33]. These results indicate that Sas3 is associated with proper cell wall biogenesis and cell wall integrity.

Preprints (www.preprints.org) | NOT PEER-REVIEWED | Posted: 8 November 2023 doi:10.20944/preprints202311.0353.v1



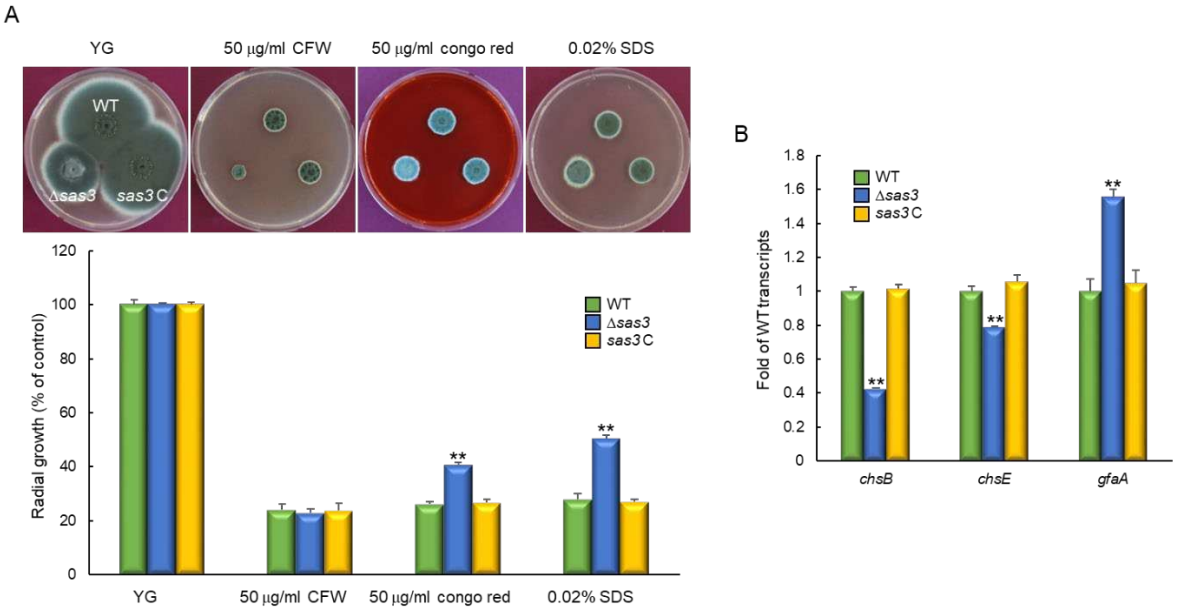


**Figure 4.** Sas3 affect sensitivity to cell wall damaging agents. (A) Colony appearance and radial growth inhibition after inoculation of 1 × $10^5$ conidia on YG containing cell wall stressors. (B) Transcript levels of the key chitin biosynthetic gene *chsB*, *chsE* and *gfaA* in the mutants and complemented strains relative to the corresponding level in the WT strain determined by RT-qPCR. The mRNA levels were normalized to the expression level of the *ef1α* gene. Statistical significance of differences was assessed by Student's *t*-test: ** $p < 0.01$.

### *3.5. Sas3 Functions in Oxidative Stress Response*

To investigate the role of Sas3 in response to oxidative stress, WT and mutant strains were incubated on YG medium supplemented with oxidative stress agents, 8 mM $H_2O_2$ and 50 μM menadione (MD). The Δ*sas3* mutant showed slightly reduced growth in response to both stress conditions (Figure 5A). To further analyze the role Sas3, we examined the activities of the ROS detoxifying enzymes. As shown in Figure 5B, activities of all catalases (CatA and Cat1) were significantly decreased in Δ*sas3* strain. All SOD activities were also considerably reduced by the loss of *sas3* (Figure 5C). These results indicate that the elevated sensitivity to external oxidative stressor of the Δ*sas3* mutant might be associated with low catalases and SODs activities.

Preprints (www.preprints.org) | NOT PEER-REVIEWED | Posted: 8 November 2023 doi:10.20944/preprints202311.0353.v1



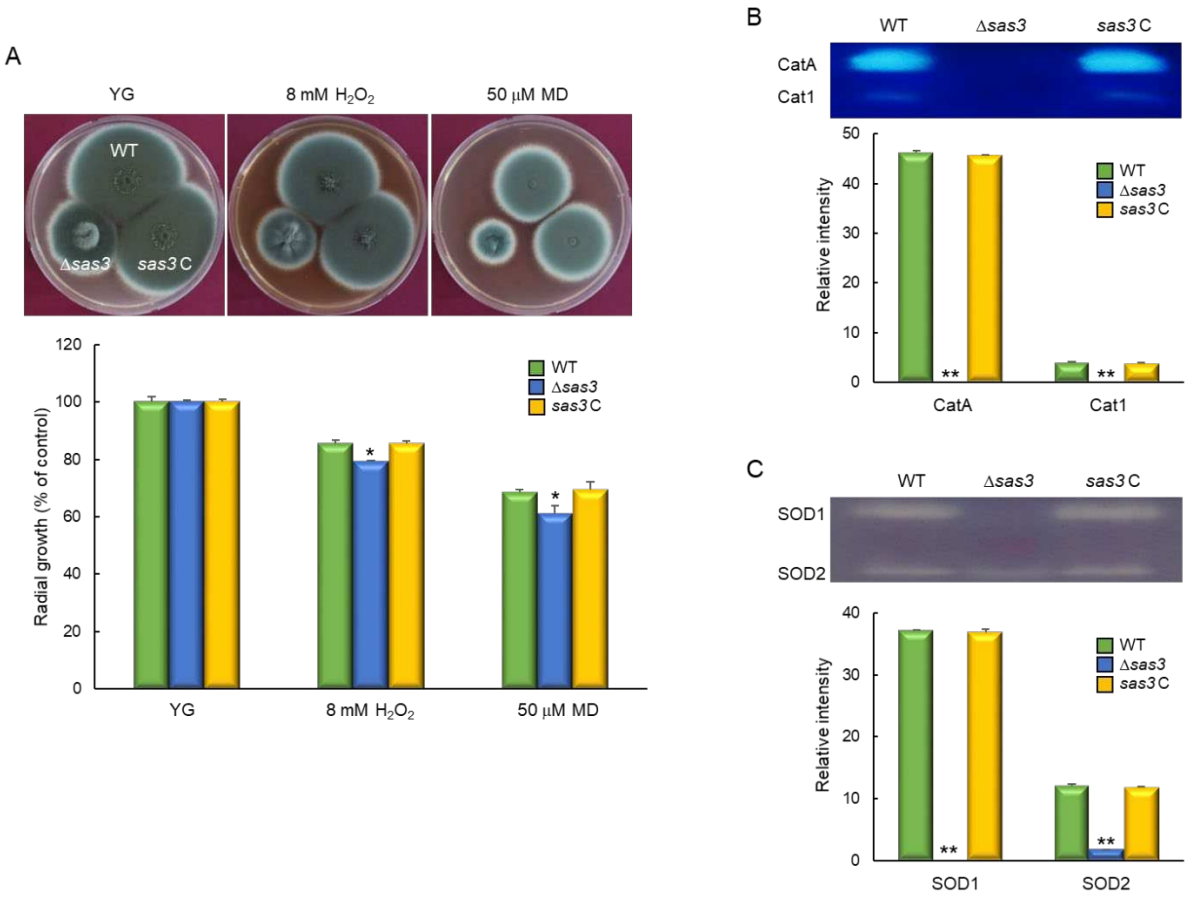


**Figure 5.** The roles of Sas3 in response to oxidative stress. (A) Colony appearance and radial growth inhibition after inoculation of $1 \times 10^5$ conidia on solid YG containing oxidative stressors. (B) Catalase activity of the WT and mutant strains. (C) SOD activity of the WT and mutant strains. Induction ratios of each enzyme's activity are shown below. Statistical significance of differences between WT and mutant strains was evaluated using Student's *t*-test: * $p < 0.05$, ** $p < 0.01$.

### *3.6. The Role of Sas3 in Fungal Virulence*

In order to assess the pathological roles of Sas3, the conidia of three strains were intranasally infected into immunocompromised mice and the pathological outcomes were analyzed by monitoring mouse survival. Mice infected with the Δ*sas3* mutant conidia survived significantly longer than those infected with the WT or *sas3* C conidia (Figure 6A). The absence of *sas3* resulted in a significantly lower pulmonary fungal burden than that of WT and *sas3* C strain (Figure 6B). Further, the interaction of conidia to murine alveolar macrophage was examined, significant decrease in phagocytosis was observed in the Δ*sas3* mutant conidia at about 132 % of the WT and *sas3* C conidia (Figure 8C). To further understand the basis for the differences in mouse survival, we performed histopathological analysis. The lung tissue sections were prepared from infected mice and stained with periodic acid–Schiff (PAS) to compare the extent of fungal impact and hyphal growth. As shown in Figure 8D, PAS staining revealed a rather small number of fungal cells in sections of the lungs infected with the Δ*sas3* mutant, which were similar to the PBS treated negative control.

Preprints (www.preprints.org) | NOT PEER-REVIEWED | Posted: 8 November 2023 doi:10.20944/preprints202311.0353.v1



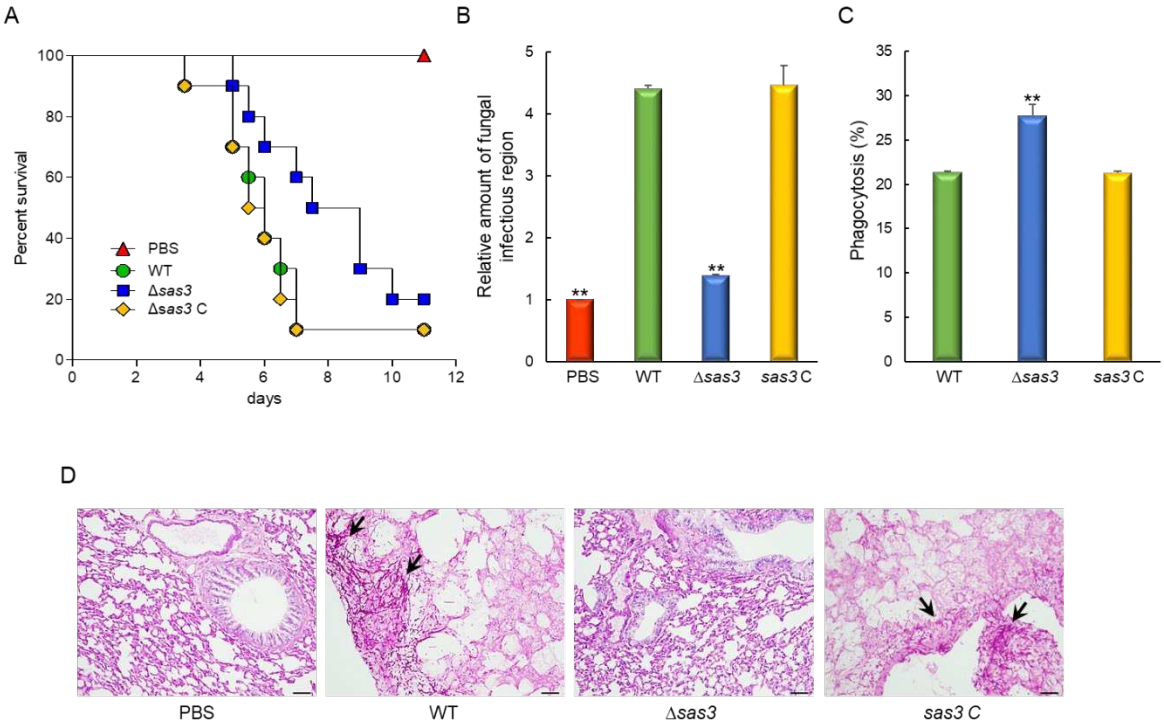


**Figure 6.** Effects of Sas3 on the virulence of *A. fumigatus*. (A) Survival curves of mice intranasally administered with conidia of WT and mutant strains ($n$ = 10/group). (B) Fungal burden in the lungs of mice infected with WT or mutant strains. (C) Phagocytosis of WT and mutant strains. Phagocytosis indicates percentage of macrophages containing one or more ingested conidia ($n$ = 20). (D) Representative lung sections of mice from different experimental groups stained with periodic acid–Schiff reagent (PAS). Arrows indicate fungal mycelium. Scale bar = 50 μm. Statistical significance of differences between WT and mutant strains was evaluated by Student's $t$-test: ** $p < 0.01$.

### *3.7. Transcriptome Analysis*

To obtain the genome-wide insight into the Sas3-mediated processes, we performed Quant-Seq (mRNA-Seq) analyses of Δ*sas3* and WT strains. Of about the 14,000,000 mapped reads, 9,833 genes differently expressed ($-1 < \log_2 FC < 1$) with 2,402 genes being significant (at least 2.0-fold, $p < 0.01$), of which 1,147 genes were up-regulated and 1,255 genes were down-regulated (Figure 7A). In molecular function gene ontology (GO) categories, "cofactor binding" and "catalytic activity" were up-regulated, whereas "signal transducer activity" and "antioxidant activity" were down-regulated. The top, up-regulated significant cellular component GO categories were "fungal-type cell wall" whereas "response to stimuli" were most down-regulated GO categories in biological process (Figure 7B). Differentially expressed genes response to stimuli are listed in Table S2. The highest up-regulated gene was predicted to encode an alternative oxidase AlxA (AFUA_2G05060) whereas the highest down-regulated gene was predicted to encode a fatty acid oxygenase (AFUA_4G00180) against external stimuli. As UV-endonuclease UVE-1 (AFUA_6G10900) was also significantly down-regulated by the loss of *sas3*, we tried to elucidate the role of Sas3 in response to UV irradiation. The expression pattern of *uve-1* transcript was first confirmed by qRT-PCR on the same RNA used for mRNA-Seq. As shown in Figure 8A, mRNA level of *uve-1* was significantly reduced in Δ*sas3* strain (0.14 fold) compared that of WT and *sas3* C strains. The radial growth of the Δ*sas3* mutant was decreased to about 85% of that of WT and *sas3* C strains in response to UV irradiation (Figure 8B). In addition, the tolerance of conidia also severely decreased against UV irradiation by the loss of *sas3* (Figure 8C).

Preprints (www.preprints.org) | NOT PEER-REVIEWED | Posted: 8 November 2023 doi:10.20944/preprints202311.0353.v1



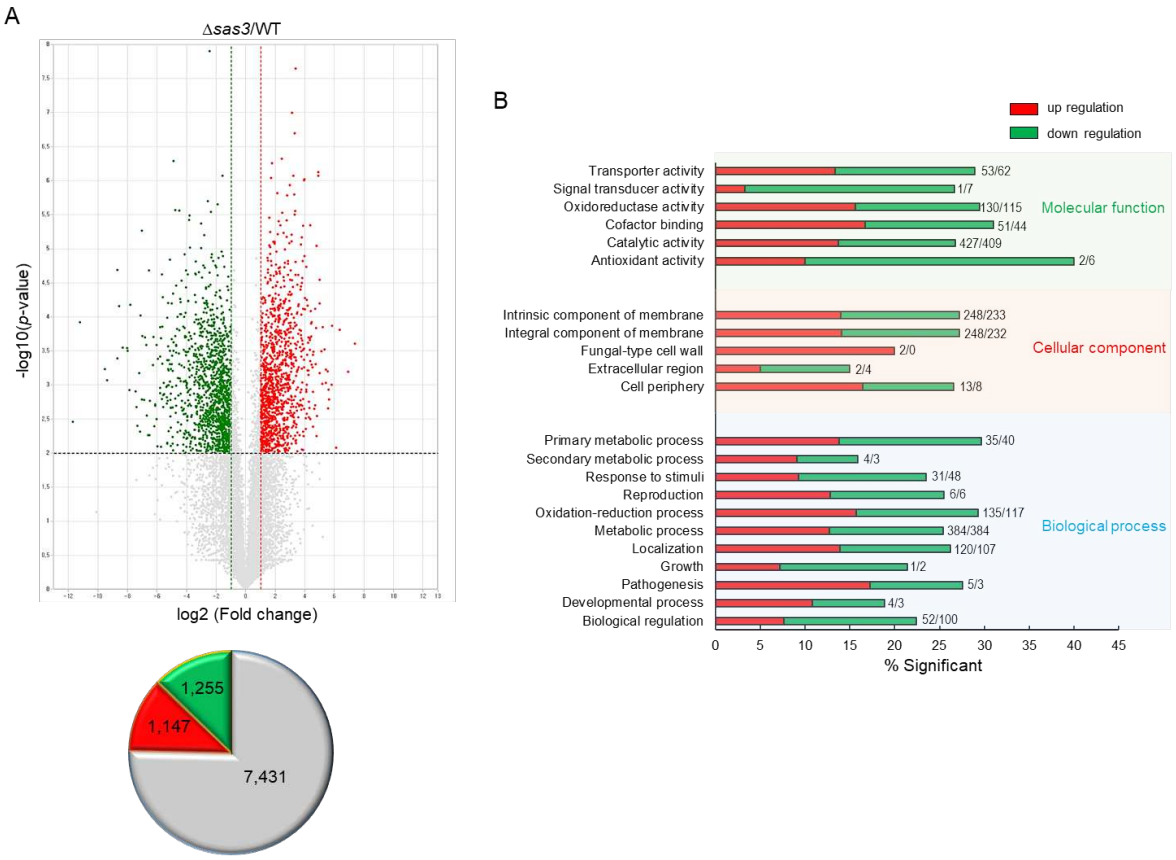


**Figure 7.** Genome-wide expression analyses of the Δ*sas3* strain. (A) Volcano plot showing the fold change (x-axis) and p-value (y-axis) of genes sequenced in Δ*sas3* strain compared to WT. Red and green dots denote up- and downregulated genes, respectively. (B) Functional annotation histograms of DEGs in Δ*sas3* strain. The red bars represent genes whose mRNA levels increased in the mutant, whereas the green bars represent those genes whose mRNA levels decreased in the mutant strain. Numbers represent significantly regulated gene number.

Preprints (www.preprints.org) | NOT PEER-REVIEWED | Posted: 8 November 2023 doi:10.20944/preprints202311.0353.v1



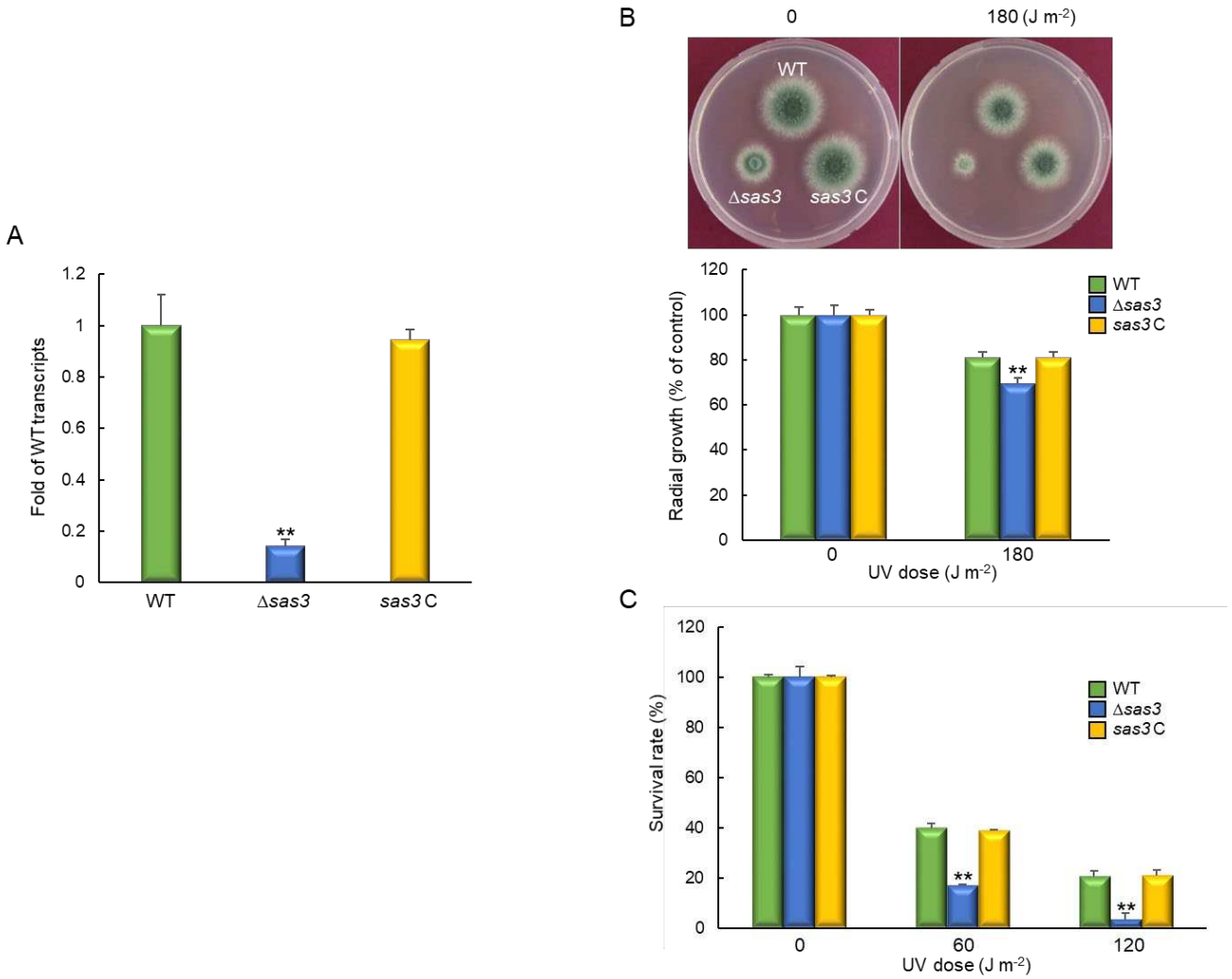


**Figure 8.** Sas3 affect tolerance against UV irradiation. (A) Expression levels of *uve-1* mRNA in WT, Δ*sas3*, and complemented (*sas3* C) strains analyzed by RT-qPCR. (B) Colony appearance and radial growth inhibition after inoculation of 1 × $10^5$ conidia on solid YG media. The plates were then irradiated immediately with UV and incubated at 37°C for 48 h. (C) Tolerance of conidia of WT, Δ*sas3*, and *sas3* C strains against UV irradiation. Statistical differences between strains were evaluated by Student's *t*-test: ** $p < 0.01$.

### *3.8. Potential Targets of Sas3*

To identify whether histone H3 acetylation levels were changed by the loss of *sas3*, we performed Western blot analyses with specific antibodies against H3acK4, H3acK9, H3acK14, H3acK18, and H3acK27, with antibodies against H3 as a loading control. In the Δ*sas3* mutant the intensities of signals for all tested antibodies were decreased compared with those of WT except for H3acK4. Especially, the signal intensities for H3acK9, H3acK14, and H3acK27 were remarkably decreased compared to those of WT (Figure 9). These results suggest that Sas3 catalyze the acetylation of lysine at the residues 9, 14, and 27 of histone H3.

Preprints (www.preprints.org) | NOT PEER-REVIEWED | Posted: 8 November 2023 doi:10.20944/preprints202311.0353.v1



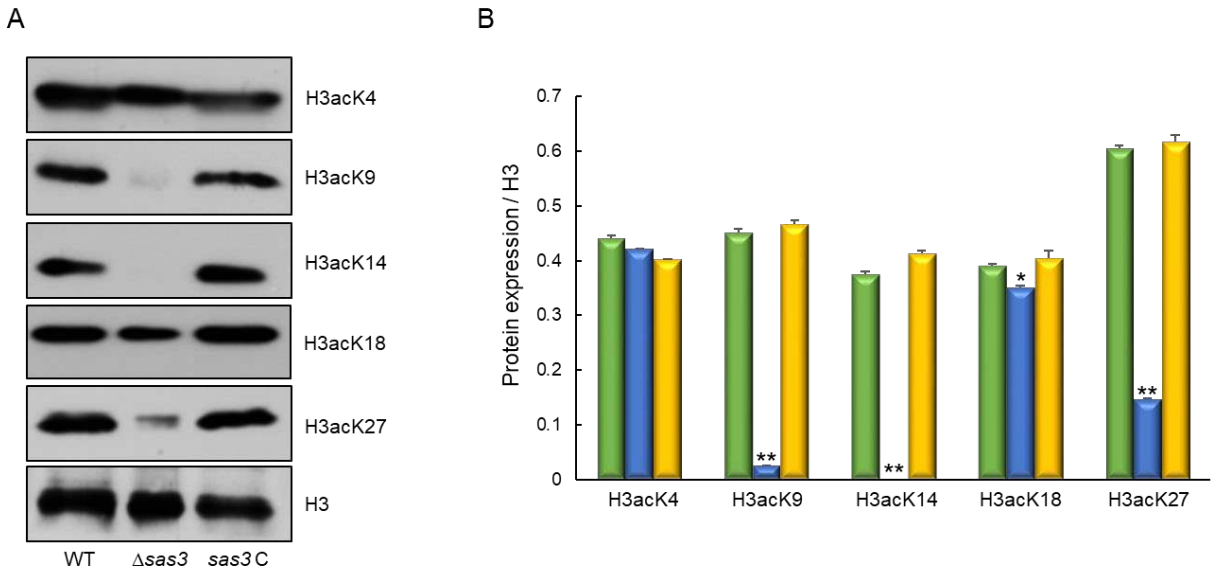


**Figure 9.** Western blot analysis of histone H3 acetylation levels. (A) The anti-acetyl H3K4 (H3acK4), anti-acetyl H3K9 (H3acK9), anti-acetyl H3K14 (H3acK14), anti-acetyl H3K18 (H3acK18), and anti-acetyl H3K27 (H3acK27) antibodies were used for the detection of alterations of acetylation levels. Antibody against H3 was used as a loading reference. (B) Quantification of Western blot signals in triplicates. Data were expressed as mean (relative to H3) ± standard error. Statistical significance of differences between WT and mutant strains was evaluated by Student's *t*-test: * $p < 0.05$, ** $p < 0.01$.

## 4. Discussion

Histone acetyltransferases (HATs) catalyze the transfer of acetyl groups from acetyl-coenzyme A onto lysine residues of core histones and commonly form part of complexes [34]. HAT complexes harbor regulatory components that regulate HAT activity and substrate specificity to prevent uncontrolled histone acetylation [35]. HATs are classified into different families, including the GNAT (Gcn5-related N-acetyltransferase) and the MYST (MOZ, YBF2/SAS3, SAS2, and TIP60) families [34]. Three MYST family of HATs were identified in human pathogenic fungus *A. fumigatus*, Esa1, Sas2, and Sas3 (dbHimo, hme.riceblast.snu.ac.kr/). Compared to the GNAT family of HATs, roles of the MYST family of HATs remains to be largely understood. In this study, we investigated the roles SAS3 of *A. fumigatus* as a MYST family HAT in fungal development and pathogenesis.

In budding yeast, the absence of *sas3* alone does not produce any remarkable phenotypic changes because Gcn5 and Sas3 have overlapping patterns of histone acetylation [36]. However, deletion of the *sas3* alone significantly impaired vegetative mycelial growth and asexual spore (conidia) production compared to the WT and *sas3* C strain. The deletion mutant not only exhibited diminished radial growth, but also exhibited reduced production of conidia, indicating Sas3 was regulated vegetative growth and asexual development. The Δ*sas3* mutant showed significantly lower PKA activity and germination rate compared to the WT and *sas3* C strains. In addition, the mutant showed the lower mRNA levels of the major components of the PKA signaling pathway, AcyA and PkaC1. These results indicate that Sas3 may negatively regulate a cAMP-PKA signaling pathway. Deletion of PKA catalytic subunit pkaC1 exhibited reduction of conidiation, vegetative growth, and pigment formation [37].

Previously, it has been demonstrated that histone acetylation plays only a minor role in the regulation of primary metabolism [38–40], but it plays an important role in secondary metabolism [41–44]. In many fungi, the production of secondary metabolites is associated with acetylation modifications of histone H3. In *A. nidulans*, the activity of several genes for secondary metabolites biosynthesis were associated with acetylation of histone H3. And the SAGA/ADA complex containing the GcnE was shown to be required for histone H3 acetylation [43]. However, there were no distinct changes in chloroform extracted secondary metabolites, including gliotoxin (GT), between

 doi:10.20944/preprints202311.0353.v1



all tested strains (Figure S2), suggesting that Sas3 plays minor roles in the regulation of secondary metabolism may be due to the absence of SAGA/ADA complex or have different mode of action in histone acetylation.

The Δ*sas3* mutant showed significantly lower virulence in a neutropenic murine model than that of WT and *sas3* C strain may be the reduction of virulence factors, such as lower resistance against oxidative stress, up-regulating phagocytosis, and resulting lower fungal burden. As a result, we found that very low spore germination and the invasion of hyphae in the lungs of mice infected with the Δ*sas3* mutant in histopathological analysis. These results indicated that Sas3-mediated histone modification involved the regulation of pathogenesis in *A. fumigatus*.

Via comparative transcriptomics analyses of WT and the Δ*sas3* mutant, mRNA levels of genes encoding the protein kinase/ribonuclease Ire1 and bZIP transcription factor HacA were significantly induced in mutant strain (Table S2). The protein kinase Ire1 has a conserved role in response to endoplasmic reticulum stress and is required for proper localization of the high-affinity iron permease Ftr1 to the cell membrane. The transcription factor HacA, which is activated by Ire1-mediated removal of the non-canonical intron in the *hacA* mRNA, is dispensable for Ftr1 localization to the cell membrane and growth under iron limiting conditions [45]. In addition, HacA plays an important roles in the unfolded protein response and required for utilization of cellulose in *Neurospora crassa* [46]. Although the expression of HacA significantly increased by the loss of *sas3*, the vegetative growth of mutant to various carbon sources, including cellulose, was slightly increased (Figure S3). The UV-endonuclease Uve-1 were significantly down-regulated by the loss of *sas3* (Table S2). The *uve-1* is a core gene regulated in response to light and responsible for tolerance against UV stress for protection of the mitochondrial genome in *C. neoformans* [47]. The results of the mRNA-Seq analysis demonstrate the diversity in cellular processes especially, utilization of carbon sources and protection against UV regulated by Sas3 in *A. fumigatus*.

Sas3 is responsible for H3K9 and H3K14 acetylation and Sas3 has overlapping patterns of H3 acetylation with Gcn5 in the budding yeast [7]. In numerous fungi, Sas3 is pivotal for the acetylation of H3K4, H3K9, H3K14, H3K18, and H3K23 [8,10]. Sas3 of *A. fumigatus* may be indispensable for the acetylation of H3K9, K3K14, and H3K29. Substrate specificities have been reported to be mediated by certain subunits from HAT complexes or HAT domains that interact with nucleosomes [48]. In *A. fumigatus*, a PHD-finger domain was identified in Sas3, with a potential role in substrate specificity or in interaction with regulatory proteins [49].

In summary, our studies have revealed that the MYST family HAT Sas3 governs diverse biological processes, such as vegetative growth, asexual sporulation, stress response, secondary metabolites production, and virulence in the human pathogenic fungus *A. fumigatus*. Revealing the crosstalk between histone modifications, their function in effector gene regulation, and the role of transcriptional activators/repressors will help us to further understand the molecular mechanisms linking chromatin and stage-specific transcriptional changes. Future work aiming to unveil global changes in histone acetylation patterns during infection will shed more light on the contribution of these histone marks to the regulation of the infection machinery.

**Supplementary Materials:** The following supporting information can be downloaded at: www.mdpi.com/xxx/s1, Figure S1: Confirmation of WT, mutants, and complemented strains; Figure S2: Roles of Sas3 and in the production of secondary metabolites; Figure S3: The effect of Sas3 on the growth in carbon sources; Table S1: Oligonucleotides used in this study; Table S2: Differentially regulated genes response to stimuli (Fold change > 2.0, $p$-value < 0.01).

**Author Contributions:** Conceptualization, J.-H.Y. and K.-S.S.; methodology, J.Y.K., Y.-H.C., and M.-W.L..; validation, M.-W.L., J.-H.Y., and K.-S.S.; investigation, J.Y.K., Y.-H.C., and M.-W.L.; data curation, M.-W.L., J.-H.Y., and K.-S.S.; writing—original draft preparation, J.-H.Y. and K.-S.S.; writ-ing—review and editing, J.-H.Y. and K.-S.S.; supervision, K.-S.S.; funding acquisition, Y.-H.C., J.-H.Y. and K.-S.S. All authors have read and agreed to the published version of the manuscript.

**Funding:** This research was funded by the National Research Foundation of Korea (NRF) grant funded by the Korea government, grant number 2020R1I1A3051661 to K.-S. Shin and 2022R1A6A3A01085818 to Y.-H. Choi. The work at UW-Madison was supported by the UW-Madison Food Research Institute.

**Institutional Review Board Statement:** All animal procedures in this study were reviewed and approved by the Institutional Animal Care and Use Committee of the Daejeon University (DJUARB2021-015; 14 June 2021).

**Informed Consent Statement:** Not applicable.

**Data Availability Statement:** RNA-Seq data are available from the NCBI Gene Expression Omnibus (GEO) database (GSE166061). The original contributions presented in the study are included in the article/Supplementary material, further inquiries can be directed to the corresponding authors.

**Conflicts of Interest:** The authors declare no conflict of interest.

## References


1. Phillips, D.M. The presence of acetyl groups of histones. *Biochem J* **1963**, *87*, 258-263, doi:10.1042/bj0870258.
2. Allfrey, V.G.; Faulkner, R.; Mirsky, A.E. Acetylation and Methylation of Histones and Their Possible Role in the Regulation of Rna Synthesis. *Proc Natl Acad Sci U S A* **1964**, *51*, 786-794, doi:10.1073/pnas.51.5.786.
3. Roth, S.Y.; Denu, J.M.; Allis, C.D. Histone acetyltransferases. *Annu Rev Biochem* **2001**, *70*, 81-120, doi:10.1146/annurev.biochem.70.1.81.
4. Jeon, J.; Kwon, S.; Lee, Y.H. Histone acetylation in fungal pathogens of plants. *Plant Pathol J* **2014**, *30*, 1-9, doi:10.5423/PPJ.RW.01.2014.0003.
5. Sapountzi, V.; Cote, J. MYST-family histone acetyltransferases: beyond chromatin. *Cell Mol Life Sci* **2011**, *68*, 1147-1156, doi:10.1007/s00018-010-0599-9.
6. Osada, S.; Sutton, A.; Muster, N.; Brown, C.E.; Yates, J.R., 3rd; Sternglanz, R.; Workman, J.L. The yeast SAS (something about silencing) protein complex contains a MYST-type putative acetyltransferase and functions with chromatin assembly factor ASF1. *Genes Dev* **2001**, *15*, 3155-3168, doi:10.1101/gad.907201.
7. John, S.; Howe, L.; Tafrov, S.T.; Grant, P.A.; Sternglanz, R.; Workman, J.L. The something about silencing protein, Sas3, is the catalytic subunit of NuA3, a yTAF(II)30-containing HAT complex that interacts with the Spt16 subunit of the yeast CP (Cdc68/Pob3)-FACT complex. *Genes Dev* **2000**, *14*, 1196-1208.
8. Chen, X.; Wu, L.; Lan, H.; Sun, R.; Wen, M.; Ruan, D.; Zhang, M.; Wang, S. Histone acetyltransferases MystA and MystB contribute to morphogenesis and aflatoxin biosynthesis by regulating acetylation in fungus *Aspergillus flavus*. *Environ Microbiol* **2022**, *24*, 1340-1361, doi:10.1111/1462-2920.15856.
9. Kong, X.; van Diepeningen, A.D.; van der Lee, T.A.J.; Waalwijk, C.; Xu, J.; Xu, J.; Zhang, H.; Chen, W.; Feng, J. The *Fusarium graminearum* Histone Acetyltransferases Are Important for Morphogenesis, DON Biosynthesis, and Pathogenicity. *Front Microbiol* **2018**, *9*, 654, doi:10.3389/fmicb.2018.00654.
10. Dubey, A.; Lee, J.; Kwon, S.; Lee, Y.H.; Jeon, J. A MYST family histone acetyltransferase, MoSAS3, is required for development and pathogenicity in the rice blast fungus. *Mol Plant Pathol* **2019**, *20*, 1491-1505, doi:10.1111/mpp.12856.
11. Fan, A.; Mi, W.; Liu, Z.; Zeng, G.; Zhang, P.; Hu, Y.; Fang, W.; Yin, W.B. Deletion of a Histone Acetyltransferase Leads to the Pleiotropic Activation of Natural Products in *Metarhizium robertsii*. *Org Lett* **2017**, *19*, 1686-1689, doi:10.1021/acs.orglett.7b00476.
12. Wang, J.J.; Cai, Q.; Qiu, L.; Ying, S.H.; Feng, M.G. The histone acetyltransferase Mst2 sustains the biological control potential of a fungal insect pathogen through transcriptional regulation. *Appl Microbiol Biotechnol* **2018**, *102*, 1343-1355, doi:10.1007/s00253-017-8703-9.
13. Xie, L.; Fang, W.; Deng, W.; Yu, Z.; Li, J.; Chen, M.; Liao, W.; Xie, J.; Pan, W. Global profiling of lysine acetylation in human histoplasmosis pathogen *Histoplasma capsulatum*. *Int J Biochem Cell Biol* **2016**, *73*, 1-10, doi:10.1016/j.biocel.2016.01.008.
14. Brandao, F.; Esher, S.K.; Ost, K.S.; Pianalto, K.; Nichols, C.B.; Fernandes, L.; Bocca, A.L.; Pocas-Fonseca, M.J.; Alspaugh, J.A. HDAC genes play distinct and redundant roles in *Cryptococcus neoformans* virulence. *Sci Rep* **2018**, *8*, 5209, doi:10.1038/s41598-018-21965-y.

15. Lin, C.J.; Hou, Y.H.; Chen, Y.L. The histone acetyltransferase GcnE regulates conidiation and biofilm formation in *Aspergillus fumigatus*. *Med Mycol* **2020**, *58*, 248-259, doi:10.1093/mmy/myz043.
16. Choi, Y.H.; Park, S.H.; Kim, S.S.; Lee, M.W.; Yu, J.H.; Shin, K.S. Functional Characterization of the GNAT Family Histone Acetyltransferase Elp3 and GcnE in *Aspergillus fumigatus*. *Int J Mol Sci* **2023**, *24*, doi:10.3390/ijms24032179.
17. Brookman, J.L.; Denning, D.W. Molecular genetics in *Aspergillus fumigatus*. *Curr Opin Microbiol* **2000**, *3*, 468-474.
18. Kafer, E. Meiotic and mitotic recombination in *Aspergillus* and its chromosomal aberrations. *Adv Genet* **1977**, *19*, 33-131.
19. Yu, J.H.; Hamari, Z.; Han, K.H.; Seo, J.A.; Reyes-Dominguez, Y.; Scazzocchio, C. Double-joint PCR: a PCR-based molecular tool for gene manipulations in filamentous fungi. *Fungal Genet Biol* **2004**, *41*, 973-981, doi:10.1016/j.fgb.2004.08.001.
20. Szewczyk, E.; Nayak, T.; Oakley, C.E.; Edgerton, H.; Xiong, Y.; Taheri-Talesh, N.; Osmani, S.A.; Oakley, B.R. Fusion PCR and gene targeting in *Aspergillus nidulans*. *Nat Protoc* **2006**, *1*, 3111-3120, doi:10.1038/nprot.2006.405.
21. Han, K.H.; Seo, J.A.; Yu, J.H. A putative G protein-coupled receptor negatively controls sexual development in *Aspergillus nidulans*. *Mol Microbiol* **2004**, *51*, 1333-1345, doi:10.1111/j.1365-2958.2003.03940.x.
22. Huan, P.; Wang, H.; Liu, B. Assessment of housekeeping genes as internal references in quantitative expression analysis during early development of oyster. *Genes Genet Syst* **2017**, *91*, 257-265, doi:10.1266/ggs.16-00007.
23. Song, H.; Dang, X.; He, Y.Q.; Zhang, T.; Wang, H.Y. Selection of housekeeping genes as internal controls for quantitative RT-PCR analysis of the veined rapa whelk (*Rapana venosa*). *PeerJ* **2017**, *5*, e3398, doi:10.7717/peerj.3398.
24. Livak, K.J.; Schmittgen, T.D. Analysis of relative gene expression data using real-time quantitative PCR and the $2^{-DDCT}$ Method. *Methods* **2001**, *25*, 402-408, doi:10.1006/meth.2001.1262.
25. Choi, Y.H.; Jun, S.C.; Lee, M.W.; Yu, J.H.; Shin, K.S. Characterization of the *mbsA* Gene Encoding a Putative APSES Transcription Factor in *Aspergillus fumigatus*. *Int J Mol Sci* **2021**, *22*, doi:10.3390/ijms22073777.
26. Lima, J.F.; Malavazi, I.; von Zeska Kress Fagundes, M.R.; Savoldi, M.; Goldman, M.H.; Schwier, E.; Braus, G.H.; Goldman, G.H. The *csnD/csnE* signalosome genes are involved in the *Aspergillus nidulans* DNA damage response. *Genetics* **2005**, *171*, 1003-1015, doi:10.1534/genetics.105.041376.
27. Lwin, H.P.; Choi, Y.H.; Lee, M.W.; Yu, J.H.; Shin, K.S. RgsA Attenuates the PKA Signaling, Stress Response, and Virulence in the Human Opportunistic Pathogen *Aspergillus fumigatus*. *Int J Mol Sci* **2019**, *20*, doi:10.3390/ijms20225628.
28. Wayne, L.G.; Diaz, G.A. A double staining method for differentiating between two classes of mycobacterial catalase in polyacrylamide electrophoresis gels. *Anal Biochem* **1986**, *157*, 89-92.
29. Weydert, C.J.; Cullen, J.J. Measurement of superoxide dismutase, catalase and glutathione peroxidase in cultured cells and tissue. *Nat Protoc* **2010**, *5*, 51-66, doi:10.1038/nprot.2009.197.
30. Beauchamp, C.; Fridovich, I. Superoxide dismutase: improved assays and an assay applicable to acrylamide gels. *Anal Biochem* **1971**, *44*, 276-287, doi:10.1016/0003-2697(71)90370-8.
31. Rocha, M.C.; Fabri, J.H.; Franco de Godoy, K.; Alves de Castro, P.; Hori, J.I.; Ferreira da Cunha, A.; Arentshorst, M.; Ram, A.F.; van den Hondel, C.A.; Goldman, G.H.; et al. *Aspergillus fumigatus* MADS-Box Transcription Factor *rlmA* Is Required for Regulation of the Cell Wall Integrity and Virulence. *G3 (Bethesda)* **2016**, *6*, 2983-3002, doi:10.1534/g3.116.031112.
32. Ibrahim-Granet, O.; Philippe, B.; Boleti, H.; Boisvieux-Ulrich, E.; Grenet, D.; Stern, M.; Latge, J.P. Phagocytosis and intracellular fate of *Aspergillus fumigatus* conidia in alveolar macrophages. *Infect Immun* **2003**, *71*, 891-903, doi:10.1128/IAI.71.2.891-903.2003.
33. Ram, A.F.; Arentshorst, M.; Damveld, R.A.; vanKuyk, P.A.; Klis, F.M.; van den Hondel, C.A. The cell wall stress response in *Aspergillus niger* involves increased expression of the glutamine : fructose-6-phosphate amidotransferase-encoding gene (*gfaA*) and increased deposition of chitin in the cell wall. *Microbiology (Reading)* **2004**, *150*, 3315-3326, doi:10.1099/mic.0.27249-0.
34. Sterner, D.E.; Berger, S.L. Acetylation of histones and transcription-related factors. *Microbiol Mol Biol Rev* **2000**, *64*, 435-459, doi:10.1128/MMBR.64.2.435-459.2000.

35. Lee, K.K.; Workman, J.L. Histone acetyltransferase complexes: one size doesn't fit all. *Nature reviews. Molecular cell biology* **2007**, *8*, 284-295, doi:10.1038/nrm2145.
36. Howe, L.; Auston, D.; Grant, P.; John, S.; Cook, R.G.; Workman, J.L.; Pillus, L. Histone H3 specific acetyltransferases are essential for cell cycle progression. *Genes Dev* **2001**, *15*, 3144-3154, doi:10.1101/gad.931401.
37. Grosse, C.; Heinekamp, T.; Kniemeyer, O.; Gehrke, A.; Brakhage, A.A. Protein kinase A regulates growth, sporulation, and pigment formation in *Aspergillus fumigatus*. *Appl Environ Microbiol* **2008**, *74*, 4923-4933, doi:10.1128/AEM.00470-08.
38. Georgakopoulos, T.; Thireos, G. Two distinct yeast transcriptional activators require the function of the GCN5 protein to promote normal levels of transcription. *EMBO J* **1992**, *11*, 4145-4152, doi:10.1002/j.1460-2075.1992.tb05507.x.
39. Reyes-Dominguez, Y.; Bok, J.W.; Berger, H.; Shwab, E.K.; Basheer, A.; Gallmetzer, A.; Scazzocchio, C.; Keller, N.; Strauss, J. Heterochromatic marks are associated with the repression of secondary metabolism clusters in *Aspergillus nidulans*. *Mol Microbiol* **2010**, *76*, 1376-1386, doi:10.1111/j.1365-2958.2010.07051.x.
40. Reyes-Dominguez, Y.; Boedi, S.; Sulyok, M.; Wiesenberger, G.; Stoppacher, N.; Krska, R.; Strauss, J. Heterochromatin influences the secondary metabolite profile in the plant pathogen *Fusarium graminearum*. *Fungal Genet Biol* **2012**, *49*, 39-47, doi:10.1016/j.fgb.2011.11.002.
41. Shwab, E.K.; Bok, J.W.; Tribus, M.; Galehr, J.; Graessle, S.; Keller, N.P. Histone deacetylase activity regulates chemical diversity in *Aspergillus*. *Eukaryot Cell* **2007**, *6*, 1656-1664, doi:10.1128/EC.00186-07.
42. Nutzmann, H.W.; Reyes-Dominguez, Y.; Scherlach, K.; Schroeckh, V.; Horn, F.; Gacek, A.; Schumann, J.; Hertweck, C.; Strauss, J.; Brakhage, A.A. Bacteria-induced natural product formation in the fungus *Aspergillus nidulans* requires Saga/Ada-mediated histone acetylation. *Proc Natl Acad Sci U S A* **2011**, *108*, 14282-14287, doi:10.1073/pnas.1103523108.
43. Nutzmann, H.W.; Fischer, J.; Scherlach, K.; Hertweck, C.; Brakhage, A.A. Distinct amino acids of histone H3 control secondary metabolism in *Aspergillus nidulans*. *Appl Environ Microbiol* **2013**, *79*, 6102-6109, doi:10.1128/AEM.01578-13.
44. Bok, J.W.; Soukup, A.A.; Chadwick, E.; Chiang, Y.M.; Wang, C.C.; Keller, N.P. VeA and MvlA repression of the cryptic orsellinic acid gene cluster in *Aspergillus nidulans* involves histone 3 acetylation. *Mol Microbiol* **2013**, *89*, 963-974, doi:10.1111/mmi.12326.
45. Ramirez-Zavala, B.; Kruger, I.; Dunker, C.; Jacobsen, I.D.; Morschhauser, J. The protein kinase Ire1 has a Hac1-independent essential role in iron uptake and virulence of *Candida albicans*. *PLoS Pathog* **2022**, *18*, e1010283, doi:10.1371/journal.ppat.1010283.
46. Montenegro-Montero, A.; Goity, A.; Larrondo, L.F. The bZIP Transcription Factor HAC-1 Is Involved in the Unfolded Protein Response and Is Necessary for Growth on Cellulose in *Neurospora crassa*. *PLoS One* **2015**, *10*, e0131415, doi:10.1371/journal.pone.0131415.
47. Verma, S.; Idnurm, A. The Uve1 endonuclease is regulated by the white collar complex to protect *Cryptococcus neoformans* from UV damage. *PLoS Genet* **2013**, *9*, e1003769, doi:10.1371/journal.pgen.1003769.
48. Eberharter, A.; Becker, P.B. Histone acetylation: a switch between repressive and permissive chromatin. Second in review series on chromatin dynamics. *EMBO reports* **2002**, *3*, 224-229, doi:10.1093/embo-reports/kvf053.
49. Kalkhoven, E.; Teunissen, H.; Houweling, A.; Verrijzer, C.P.; Zantema, A. The PHD type zinc finger is an integral part of the CBP acetyltransferase domain. *Mol Cell Biol* **2002**, *22*, 1961-1970, doi:10.1128/MCB.22.7.1961-1970.2002.